

# WAVELETS: MATHEMATICS AND APPLICATIONS

I.M. Dremin<sup>1</sup>

*Lebedev Physical Institute, Moscow 119991, Russia*

## Abstract

The notion of wavelets is defined. It is briefly described *what* are wavelets, *how* to use them, *when* we do need them, *why* they are preferred and *where* they have been applied. Then one proceeds to the multiresolution analysis and fast wavelet transform as a standard procedure for dealing with discrete wavelets. It is shown which specific features of signals (functions) can be revealed by this analysis, but can not be found by other methods (e.g., by the Fourier expansion). Finally, some examples of practical application are given. Rigorous proofs of mathematical statements are omitted, and the reader is referred to the corresponding literature.

## 1 Introduction

Let us define wavelets as a complete orthonormal system of functions with a compact support obtained with the help of dilations and translations. Sometimes a wider class of functions is also called "wavelets" if the properties of completeness and/or orthonormality are not required. In what follows, we will use the so-called discrete wavelets satisfying above rigorous definition.

Wavelets have become a necessary mathematical tool in many investigations. They are used in those cases when the result of the analysis of a particular *signal*<sup>2</sup> should contain not only the list of its typical frequencies (scales) but also a definite knowledge of the particular local coordinates where these properties are important. Thus, analysis and processing of different classes of nonstationary (in time) or inhomogeneous (in space) signals is the main field of applications of wavelet analysis .

In particle physics, wavelets can be used for analysis of multiparticle production processes, for separation of close overlapping resonances, for revealing small fluctuations over huge background etc. The inhomogeneity of the secondary particle distributions in the available phase space is one of the fields of wavelet applications as demonstrated below. Beside their application to analysis of experimental data, wavelets can be successfully used for computer solution of non-linear equations because they provide very effective and stable basis, especially for expansions in equations containing many varying scales.

The wavelet basis is formed by using dilations and translations of a particular function defined on a finite interval. Its finiteness is crucial for the locality property of the wavelet analysis . Commonly used (so-called discrete) wavelets generate a complete orthonormal system of functions with a finite support constructed in such a way. That is why by changing the scale (dilations) they can distinguish the local characteristics of a signal at various scales, and by translations they cover the whole region in which it is studied. Due to the completeness of the system, they also allow for the inverse transformation to be properly done. In the analysis of nonstationary signals, the locality property of wavelets gives a substantial advantage over Fourier transform which provides us only with knowledge of the global frequencies (scales) of the object under investigation because

---

<sup>1</sup>Email: dremin@lpi.ru

<sup>2</sup>The notion of a signal is used here for any ordered set of numerically recorded information about some processes, objects, functions etc. The signal can be a function of some coordinates, would it be the time, the space or any other (in general,  $n$ -dimensional) scale.

the system of the basic functions used (sine, cosine or imaginary exponential functions) is defined over an infinite interval.

The literature devoted to wavelets is very extensive, and one can easily get a lot of references by sending the corresponding request to Internet web sites. Mathematical problems are treated in many monographs in detail (e.g., see [1, 2, 3, 4, 5]). Introductory courses on wavelets can be found in the books [6, 7, 8, 9]. The review papers adapted for physicists and practical users were published in Physics-Uspekhi journal [10, 11] and are available from website [www.ufn.ru](http://www.ufn.ru), see also [www.awavelet.ru](http://www.awavelet.ru). In particular, this talk delivered at the session of RAN is mainly based on the review paper [11].

It has been proven that any function can be written as a superposition of wavelets, and there exists a numerically stable algorithm to compute the coefficients for such an expansion. Moreover, these coefficients completely characterize the function, and it is possible to reconstruct it in a numerically stable way if these coefficients have been determined. Because of their unique properties, wavelets were used in functional analysis in mathematics, in studies of (multi)fractal properties, singularities and local oscillations of functions, for solving some differential equations, for investigation of inhomogeneous processes involving widely different scales of interacting perturbations, for noise analysis, for pattern recognition, for image and sound compression, for digital geometry processing, for solving many problems of physics, biology, medicine, technique etc (see the recently published books [12, 13, 14, 15]). This list is by no means exhaustive.

The codes exploiting the wavelet transform are widely used now not only for scientific research but for commercial projects as well. Some of them have been even described in books (e.g., see [16]). At the same time, the direct transition from pure mathematics to computer programming and applications is non-trivial and asks often for the individual approach to the problem under investigation and for a specific choice of wavelets used. Our main objective here is to describe in a suitable way the bridge that relates mathematical wavelet constructions to practical signal processing. Practical applications considered by A. Grossman and J. Morlet [17, 18] have led to fast progress of the wavelet theory related to the work of Y. Meyer, I. Daubechies et al.

The main bulk of papers dealing with practical applications of wavelet analysis uses the so-called discrete wavelets which will be our main concern here. The discrete wavelets look strange to those accustomed to analytical calculations because they can not be represented by analytical expressions (except for the simplest one) or by solutions of some differential equations, and instead are given numerically as solutions of definite functional equations containing rescaling and translations. Moreover, in practical calculations their direct form is not even required, and only the numerical values of the coefficients of the functional equation are used. Thus the wavelet basis is defined by the iterative algorithm of the dilation and translation of a single function. This leads to a very important procedure called multiresolution analysis which gives rise to the multiscale local analysis of the signal and fast numerical algorithms. Each scale contains an independent non-overlapping set of information about the signal in the form of wavelet coefficients, which are determined from an iterative procedure called the fast wavelet transform. In combination, they provide its complete *analysis* and simplify the *diagnosis* of the underlying processes.

After such an analysis has been done, one can *compress* (if necessary) the resulting data by omitting some inessential part of the *encoded* information. This is done with the help of the so-called *quantization* procedure which commonly allocates different weights to various wavelet coefficients obtained. In particular, it helps erase some statistical fluctuations and, therefore, increase the role of the dynamical features of a signal. This can however falsify the diagnostic if the compression is done inappropriately. Usually, accurate compression gives rise to a substantial reduction of the required computer *storage* memory and *transmission* facilities, and, consequently,

to a lower expenditure. The number of vanishing moments of wavelets is important at this stage. Unfortunately, the compression introduces unavoidable systematic errors. The mistakes one has made will consist of multiples of the deleted wavelet coefficients, and, therefore, the regularity properties of a signal play an essential role. *Reconstruction* after such compression schemes is then no longer perfect. These two objectives are clearly antagonistic. Nevertheless, when one tries to reconstruct the initial signal, the inverse transformation (*synthesis*) happens to be rather stable and reproduces its most important characteristics if proper methods are applied. The regularity properties of wavelets used also become crucial at the reconstruction stage. The distortions of the reconstructed signal due to quantization can be kept small, although significant compression ratios are attained. Since the part of the signal which is not reconstructed is often called noise, in essence, what we are doing is denoising the signals. Namely at this stage the superiority of the discrete wavelets becomes especially clear.

Thus, the objectives of signal processing consist in accurate analysis with help of the transform, effective coding, fast transmission and, finally, careful reconstruction (at the transmission destination point) of the initial signal. Sometimes the first stage of signal analysis and diagnosis is enough for the problem to be solved and the anticipated goals to be achieved.

One should however stress that, even though this method is very powerful, the goals of wavelet analysis are rather modest. This helps us describe and reveal some features, otherwise hidden in a signal, but it does not pretend to explain the underlying dynamics and physical origin although it may give some crucial hints to it. Wavelets present a new stage in optimization of this description providing, in many cases, the best known representation of a signal. With the help of wavelets, we merely see things a little more clearly.

However, one should not underestimate the significance of information obtained by this analysis. It often provides such new knowledge of processes otherwise hidden but underlying the crucial dynamics which can not be found from traditional approaches. This helps further introduce models assumed to be driving the mechanisms generating the observations and, therefore, to get deeper insight into the dynamics of the processes.

To define the optimality of the algorithms of the wavelet transform, some (still debatable!) energy and entropy criteria have been developed. They are internal to the algorithm itself. However, the choice of the best algorithm is also tied to the objective goal of its practical use, i.e., to some external criteria. That is why in practical applications one should submit the performance of a "theoretically optimal algorithm" to the judgements of experts and users to estimate its advantage over the previously developed ones.

Despite very active research and impressive results, the versatility of wavelet analysis implies that these studies are presumably not in their final form yet. We shall try to describe the situation in its *status nascendi*.

## 2 Wavelets for beginners

Each signal can be characterized by its averaged (over some intervals) values (trend) and by its variations around this trend. Let us call these variations as fluctuations independently of their nature, be they of dynamic, stochastic, psychological, physiological or any other origin. When processing a signal, one is interested in its fluctuations at various scales because from these one can learn about their origin. The goal of wavelet analysis is to provide tools for such processing.

Actually, physicists dealing with experimental histograms analyze their data at different scales when averaging over different size intervals. This is a particular example of a simplified wavelet

analysis treated in this Section. To be more definite, let us consider the situation when an experimentalist measures some function  $f(x)$  within the interval  $0 \leq x \leq 1$ , and the best resolution obtained with the measuring device is limited by 1/16th of the whole interval. Thus the result consists of 16 numbers representing the mean values of  $f(x)$  in each of these bins and can be plotted as a 16-bin histogram shown in the upper part of Fig. 1. It can be represented by the following formula

$$f(x) = \sum_{k=0}^{15} s_{4,k} \varphi_{4,k}(x), \quad (1)$$

where  $s_{4,k} = f(k/16)/4$ , and  $\varphi_{4,k}$  is defined as a step-like block of the unit norm (i.e. of height 4 and widths 1/16) different from zero only within the  $k$ -th bin. For an arbitrary  $j$ , one imposes the condition  $\int dx |\varphi_{j,k}|^2 = 1$ , where the integral is taken over the intervals of the lengths  $\Delta x_j = 1/2^j$  and, therefore,  $\varphi_{j,k}$  have the following form  $\varphi_{j,k} = 2^{j/2} \varphi(2^j x - k)$  with  $\varphi$  denoting a step-like function of the unit height over such an interval. The label 4 is related to the total number of such intervals in our example. At the next coarser level the average over the two neighboring bins is taken as is depicted in the histogram just below the initial one in Fig. 1. Up to the normalization factor, we will denote it as  $s_{3,k}$  and the difference between the two levels shown to the right of this histogram as  $d_{3,k}$ . To be more explicit, let us write down the normalized sums and differences for an arbitrary level  $j$  as

$$s_{j-1,k} = \frac{1}{\sqrt{2}} [s_{j,2k} + s_{j,2k+1}]; \quad d_{j-1,k} = \frac{1}{\sqrt{2}} [s_{j,2k} - s_{j,2k+1}], \quad (2)$$

or for the backward transform (synthesis)

$$s_{j,2k} = \frac{1}{\sqrt{2}} (s_{j-1,k} + d_{j-1,k}); \quad s_{j,2k+1} = \frac{1}{\sqrt{2}} (s_{j-1,k} - d_{j-1,k}). \quad (3)$$

Since, for the dyadic partition considered, this difference has opposite signs in the neighboring bins of the previous fine level, we introduce the function  $\psi$  which is 1 and -1, correspondingly, in these bins and the normalized functions  $\psi_{j,k} = 2^{j/2} \psi(2^j x - k)$ . This allows us to represent the same function  $f(x)$  as

$$f(x) = \sum_{k=0}^7 s_{3,k} \varphi_{3,k}(x) + \sum_{k=0}^7 d_{3,k} \psi_{3,k}(x). \quad (4)$$

One proceeds further in the same manner to the sparser levels 2, 1 and 0 with averaging done over the interval lengths 1/4, 1/2 and 1, correspondingly. This is shown in the subsequent drawings in Fig. 1. The most sparse level with the mean value of  $f$  over the whole interval denoted as  $s_{0,0}$  provides

$$f(x) = s_{0,0} \varphi_{0,0}(x) + d_{0,0}(x) \psi_{0,0}(x) + \sum_{k=0}^1 d_{1,k} \psi_{1,k}(x) + \sum_{k=0}^3 d_{2,k} \psi_{2,k}(x) + \sum_{k=0}^7 d_{3,k} \psi_{3,k}(x). \quad (5)$$

The functions  $\varphi_{0,0}(x)$  and  $\psi_{0,0}(x)$  are shown in Fig. 2. The functions  $\varphi_{j,k}(x)$  and  $\psi_{j,k}(x)$  are normalized by the conservation of the norm, dilated and translated versions of them. In the next Section we will give explicit formulae for them in a particular case of Haar scaling functions and wavelets. In practical signal processing, these functions (and more sophisticated versions of them)

are often called low and high-path filters, correspondingly, because they filter the large and small scale components of a signal. The subsequent terms in Eq. (5) show the fluctuations (differences  $d_{j,k}$ ) at finer and finer levels with larger  $j$ . In all the cases (1)–(5) one needs exactly 16 coefficients to represent the function. In general, there are  $2^j$  coefficients  $s_{j,k}$  and  $2^{j_n} - 2^j$  coefficients  $d_{j,k}$ , where  $j_n$  denotes the finest resolution level (in the above example,  $j_n = 4$ ).

All the above representations of the function  $f(x)$  (Eqs. (1)–(5)) are mathematically equivalent. However, the latter one representing the wavelet analyzed function directly reveals the fluctuation structure of the signal at different scales  $j$  and various locations  $k$  present in a set of coefficients  $d_{j,k}$  whereas the original form (1) hides the fluctuation patterns in the background of a general trend. The final form (5) contains the overall average of the signal depicted by  $s_{0,0}$  and all its fluctuations with their scales and positions well labelled by 15 normalized coefficients  $d_{j,k}$  while the initial histogram shows only the normalized average values  $s_{j,k}$  in the 16 bins studied. Moreover, in practical applications the latter wavelet representation is preferred because for rather smooth functions, strongly varying only at some discrete values of their arguments, many of the high-resolution  $d$ -coefficients in relations similar to Eq. (5) are close to zero (compared to the "informative"  $d$ -coefficients) and can be discarded. Bands of zeros (or close to zero values) indicate those regions where the function is fairly smooth.

At first sight, this simplified example looks somewhat trivial. However, for more complicated functions and more data points with some elaborate forms of wavelets it leads to a detailed analysis of a signal and to possible strong compression with subsequent good quality restoration. This example also provides an illustration of the very important feature of the whole approach with successive coarser and coarser approximations to  $f$  called the multiresolution analysis and discussed in more detail below.

### 3 Basic notions and Haar wavelets

To analyze any signal, one should, first of all, choose the corresponding basis, i.e., the set of functions to be considered as "functional coordinates". In most cases we will deal with signals represented by the square integrable functions defined on the real axis. They form the infinite-dimensional Hilbert space  $L^2(R)$ . For nonstationary signals, e.g., the location of that moment when the frequency characteristics has abruptly been changed is crucial. Therefore the basis should have a compact support. The wavelets are just such functions which span the whole space by translation of the dilated versions of a definite function. That is why every signal can be decomposed in the wavelet series (or integral). Each frequency component is studied with a resolution matched to its scale.

Let us try to construct functions satisfying the above criteria. An educated guess would be to relate the function  $\varphi(x)$  to its dilated and translated version. The simplest linear relation with  $2M$  coefficients is

$$\varphi(x) = \sqrt{2} \sum_{k=0}^{2M-1} h_k \varphi(2x - k) \quad (6)$$

with the dyadic dilation 2 and integer translation  $k$ . At first sight, the chosen normalization of the coefficients  $h_k$  with the "extracted" factor  $\sqrt{2}$  looks somewhat arbitrary. Actually, it is defined *a posteriori* by the traditional form of fast algorithms for their calculation (see Eqs. (34) and (35) below) and normalization of functions  $\varphi_{j,k}(x), \psi_{j,k}(x)$ . It is used in all the books cited above. However, sometimes (see [2], Chapter 7) it is replaced by  $c_k = \sqrt{2}h_k$ .

For discrete values of the dilation and translation parameters one gets discrete wavelets. The value of the dilation factor determines the size of cells in the lattice chosen. The integer  $M$  defines the number of coefficients and the length of the wavelet support. They are interrelated because from the definition of  $h_k$  for orthonormal bases

$$h_k = \sqrt{2} \int dx \varphi(x) \bar{\varphi}(2x - k) \quad (7)$$

it follows that only finitely many  $h_k$  are nonzero if  $\varphi$  has a finite support. The normalization condition is chosen as

$$\int_{-\infty}^{\infty} dx \varphi(x) = 1. \quad (8)$$

The function  $\varphi(x)$  obtained from the solution of this equation is called a scaling function<sup>3</sup>. If the scaling function is known, one can form a "mother wavelet" (or a basic wavelet)  $\psi(x)$  according to

$$\psi(x) = \sqrt{2} \sum_{k=0}^{2M-1} g_k \varphi(2x - k), \quad (9)$$

where

$$g_k = (-1)^k h_{2M-k-1}. \quad (10)$$

The simplest example would be for  $M = 1$  with two non-zero coefficients  $h_k$  equal to  $1/\sqrt{2}$ , i.e., the equation leading to the Haar scaling function  $\varphi_H(x)$ :

$$\varphi_H(x) = \varphi_H(2x) + \varphi_H(2x - 1). \quad (11)$$

One easily gets the solution of this functional equation

$$\varphi_H(x) = \theta(x)\theta(1 - x), \quad (12)$$

where  $\theta(x)$  is the Heaviside step-function equal to 1 at positive arguments and 0 at negative ones. The additional boundary condition is  $\varphi_H(0) = 1$ ,  $\varphi_H(1) = 0$ . This condition is important for the simplicity of the whole procedure of computing the wavelet coefficients when two neighboring intervals are considered.

The "mother wavelet" is

$$\psi_H(x) = \theta(x)\theta(1 - 2x) - \theta(2x - 1)\theta(1 - x). \quad (13)$$

with boundary values defined as  $\psi_H(0) = 1$ ,  $\psi_H(1/2) = -1$ ,  $\psi_H(1) = 0$ . This is the Haar wavelet [19] known since 1910 and used in the functional analysis. Both the scaling function  $\varphi_H(x)$  and the "mother wavelet"  $\psi_H(x)$  are shown in Fig. 2. This is the first one of a family of compactly supported orthonormal wavelets  $M\psi : \psi_H =_1 \psi$ . It possesses the locality property since its support  $2M - 1 = 1$  is compact. Namely this example has been considered in the previous Section for the histogram decomposition. It is easily seen that each part of a histogram is composed of a combination of a scaling function and a wavelet with corresponding weights considered at a definite scale.

The dilated and translated versions of the scaling function  $\varphi$  and the "mother wavelet"  $\psi$

$$\varphi_{j,k} = 2^{j/2} \varphi(2^j x - k), \quad (14)$$

---

<sup>3</sup>It is often called also a "father wavelet" but we will not use this term.

$$\psi_{j,k} = 2^{j/2}\psi(2^j x - k) \quad (15)$$

form the orthonormal basis as can be (easily for Haar wavelets) checked<sup>4</sup>. The choice of  $2^j$  with the integer valued  $j$  as a scaling factor leads to the unique and selfconsistent procedure of computing the wavelet coefficients. Integer values of  $j$  are in charge of the name "discrete" used for this set of wavelets.

The Haar wavelet oscillates so that

$$\int_{-\infty}^{\infty} dx\psi(x) = 0. \quad (16)$$

This condition is common for all the wavelets. It is called the oscillation or cancellation condition. From it, the origin of the name wavelet becomes clear. One can describe a "wavelet" as a function that oscillates within some interval like a wave but is then localized by damping outside this interval. This is a necessary condition for wavelets to form an unconditional (stable) basis. We conclude that for special choices of coefficients  $h_k$  one gets the specific forms of "mother" wavelets, which give rise to orthonormal bases.

One may decompose any function  $f$  of  $L^2(R)$  at any resolution level  $j_n$  in a series

$$f = \sum_k s_{j_n,k}\varphi_{j_n,k} + \sum_{j \geq j_n,k} d_{j,k}\psi_{j,k}. \quad (17)$$

At the finest resolution level  $j_n = j_{max}$  only  $s$ -coefficients are left, and one gets the scaling-function representation

$$f(x) = \sum_k s_{j_{max},k}\varphi_{j_{max},k}. \quad (18)$$

In the case of the Haar wavelets it corresponds to the initial experimental histogram with the finest resolution. Since we will be interested in its analysis at varying resolutions, this form is used as an initial input only. The final representation of the same data (17) shows all the fluctuations in the signal. The wavelet coefficients  $s_{j,k}$  and  $d_{j,k}$  can be calculated as

$$s_{j,k} = \int dx f(x)\varphi_{j,k}(x), \quad (19)$$

$$d_{j,k} = \int dx f(x)\psi_{j,k}(x). \quad (20)$$

However, in practice their values are determined from the fast wavelet transform described below.

In reference to the particular case of the Haar wavelet, considered above, these coefficients are often referred as sums ( $s$ ) and differences ( $d$ ), thus related to mean values and fluctuations.

Only the second term in (17) is often considered, and the result is often called as the wavelet expansion. For the histogram interpretation, the neglect of first sum would imply that one is not interested in average values but only in the histogram shape determined by fluctuations at different scales. Any function can be approximated to a precision  $2^{j/2}$  (i.e., to an arbitrary high precision at  $j \rightarrow -\infty$ ) by a finite linear combination of Haar wavelets.

---

<sup>4</sup>We return back to the general case and therefore omit the index  $H$  because the same formula will be used for other wavelets.

## 4 Multiresolution analysis and Daubechies wavelets

Though the Haar wavelets provide a good tutorial example of an orthonormal basis, they suffer from several deficiencies. One of them is the bad analytic behavior with the abrupt change at the interval bounds, i.e., its bad regularity properties. By this we mean that all finite rank moments of the Haar wavelet are different from zero - only its zeroth moment, i.e., the integral (16) of the function itself is zero. This shows that this wavelet is not orthogonal to any polynomial apart from a trivial constant. The Haar wavelet does not have good time-frequency localization. Its Fourier transform decays like  $|\omega|^{-1}$  for  $\omega \rightarrow \infty$ .

The goal is to find a general class of those functions which would satisfy the requirements of locality, regularity and oscillatory behavior. They should be simple enough in the sense that they are of being sufficiently explicit and regular to be completely determined by their samples on the lattice defined by the factors  $2^j$ .

The general approach which respects these properties is known as the multiresolution approximation. A rigorous mathematical definition is given in the abovecited monographs. One can define the notion of wavelets so that the functions  $2^{j/2}\psi(2^jx - k)$  are the wavelets (generated by the "mother"  $\psi$ ), possessing the regularity, the localization and the oscillation properties. By varying  $j$  we can resolve signal properties at different scales, while  $k$  shows the location of the analyzed region.

We just show how the program of the multiresolution analysis works in practice when applied to the problem of finding out the coefficients of any filter  $h_k$  and  $g_k$ . They can be directly obtained from the definition and properties of the discrete wavelets. These coefficients are defined by relations (6) and (9)

$$\varphi(x) = \sqrt{2} \sum_k h_k \varphi(2x - k); \quad \psi(x) = \sqrt{2} \sum_k g_k \varphi(2x - k), \quad (21)$$

where  $\sum_k |h_k|^2 < \infty$ . The orthogonality of the scaling functions defined by the relation

$$\int dx \varphi(x) \varphi(x - m) = 0 \quad (22)$$

leads to the following equation for the coefficients:

$$\sum_k h_k h_{k+2m} = \delta_{0m}. \quad (23)$$

The orthogonality of wavelets to the scaling functions

$$\int dx \psi(x) \varphi(x - m) = 0 \quad (24)$$

gives the equation

$$\sum_k h_k g_{k+2m} = 0, \quad (25)$$

having a solution of the form

$$g_k = (-1)^k h_{2M-1-k}. \quad (26)$$

Thus the coefficients  $g_k$  for wavelets are directly defined by the scaling function coefficients  $h_k$ .

Another condition of the orthogonality of wavelets to all polynomials up to the power  $(M-1)$  (thus, to any noise described by such polynomials), defining its regularity and oscillatory behavior

$$\int dx x^n \psi(x) = 0, \quad n = 0, \dots, (M-1), \quad (27)$$



provides the relation

$$\sum_k k^n g_k = 0, \quad (28)$$

giving rise to

$$\sum_k (-1)^k k^n h_k = 0, \quad (29)$$

when the formula (26) is taken into account.

The normalization condition

$$\int dx \varphi(x) = 1 \quad (30)$$

can be rewritten as another equation for  $h_k$ :

$$\sum_k h_k = \sqrt{2}. \quad (31)$$

Let us write down the equations (23),(29), (31) for  $M = 2$  explicitly:

$$\begin{aligned} h_0 h_2 + h_1 h_3 &= 0, \\ h_0 - h_1 + h_2 - h_3 &= 0, \\ -h_1 + 2h_2 - 3h_3 &= 0, \\ h_0 + h_1 + h_2 + h_3 &= \sqrt{2}. \end{aligned}$$

The solution of this system is

$$h_3 = \frac{1}{4\sqrt{2}}(1 \pm \sqrt{3}), \quad h_2 = \frac{1}{2\sqrt{2}} + h_3, \quad h_1 = \frac{1}{\sqrt{2}} - h_3, \quad h_0 = \frac{1}{2\sqrt{2}} - h_3, \quad (32)$$

that, in the case of the minus sign for  $h_3$ , corresponds to the well known filter

$$h_0 = \frac{1}{4\sqrt{2}}(1 + \sqrt{3}), \quad h_1 = \frac{1}{4\sqrt{2}}(3 + \sqrt{3}), \quad h_2 = \frac{1}{4\sqrt{2}}(3 - \sqrt{3}), \quad h_3 = \frac{1}{4\sqrt{2}}(1 - \sqrt{3}). \quad (33)$$

These coefficients define the simplest  $D^4$  (or  ${}_2\psi$ ) wavelet from the famous family of orthonormal Daubechies wavelets with finite support. It is shown in the upper part of Fig. 3 by the dotted line with the corresponding scaling function shown by the solid line. Some other higher rank wavelets are also shown there. It is clear from this Figure (especially, for  $D^4$ ) that wavelets are smoother at some points than at others.

For the filters of higher order in  $M$ , i.e., for higher rank Daubechies wavelets, the coefficients can be obtained in an analogous manner. The wavelet support is equal to  $2M - 1$ . It is wider than for the Haar wavelets. However the regularity properties are better. The higher order wavelets are smoother compared to  $D^4$  as seen in Fig. 3.

## 5 Fast wavelet transform

The coefficients  $s_{j,k}$  and  $d_{j,k}$  carry information about the content of the signal at various scales and can be calculated directly using the formulas (19), (20). However this algorithm is inconvenient for numerical computations because it requires many ( $N^2$ ) operations where  $N$  denotes a number of the sampled values of the function. In practical calculations the coefficients  $h_k$  are used only without referring to the shapes of wavelets.

In real situations with digitized signals, we have to deal with finite sets of points. Thus, there always exists the finest level of resolution where each interval contains only a single number. Correspondingly, the sums over  $k$  will get finite limits. It is convenient to reverse the level indexation assuming that the label of this fine scale is  $j = 0$ . It is then easy to compute the wavelet coefficients for more sparse resolutions  $j \geq 1$ .

Multiresolution analysis naturally leads to an hierarchical and fast scheme for the computation of the wavelet coefficients of a given function. The functional equations (6), (9) and the formulas for the wavelet coefficients (19), (20) give rise, in the case of Haar wavelets, to the relations (2), or for the backward transform (synthesis) to (3).

In general, one can get the iterative formulas of the fast wavelet transform

$$s_{j+1,k} = \sum_m h_m s_{j,2k+m}, \quad (34)$$

$$d_{j+1,k} = \sum_m g_m s_{j,2k+m} \quad (35)$$

where

$$s_{0,k} = \int dx f(x) \varphi(x - k). \quad (36)$$

These equations yield fast (so-called pyramid) algorithm for computing the wavelet coefficients, asking now just for  $O(N)$  operations to be done. Starting from  $s_{0,k}$ , one computes all other coefficients provided the coefficients  $h_m$ ,  $g_m$  are known. The explicit shape of the wavelet is not used in this case any more.

The remaining problem lies in the initial data. If an explicit expression for  $f(x)$  is available, the coefficients  $s_{0,k}$  may be evaluated directly according to (36). But this is not so in the situation when only discrete values are available. In the simplest approach they are chosen as  $s_{0,k} = f(k)$ .

## 6 The Fourier and wavelet transforms

The wavelet transform is superior to the Fourier transform, first of all, due to the locality property of wavelets. The Fourier transform uses sine, cosine or imaginary exponential functions as the main basis. It is spread over the entire real axis whereas the wavelet basis is localized. An attempt to overcome these difficulties and improve time-localization while still using the same basis functions is made by the so-called windowed Fourier transform. The signal  $f(t)$  is considered within some time interval (window) only. However, all windows have the same width.

In contrast, the wavelets  $\psi$  automatically provide the time (or spatial location) resolution window adapted to the problem studied, i.e., to its essential frequencies (scales). Namely, let  $t_0$ ,  $\delta$  and  $\omega_0$ ,  $\delta_\omega$  be the centers and the effective widths of the wavelet basic function  $\psi(t)$  and its Fourier transform. Then for the wavelet family  $\psi_{j,k}(t)$  (15) and, correspondingly, for wavelet coefficients, the center and the width of the window along the  $t$ -axis are given by  $2^j(t_0 + k)$  and  $2^j\delta$ . Along the  $\omega$ -axis they are equal to  $2^{-j}\omega_0$  and  $2^{-j}\delta_\omega$ . Thus the ratios of widths to the center position along each axis do not depend on the scale. This means that the wavelet window resolves both the location and the frequency in fixed proportions to their central values. For the high-frequency component of the signal it leads to a quite large frequency extension of the window whereas the time location interval is squeezed so that the Heisenberg uncertainty relation is not violated. That is why wavelet windows can be called Heisenberg windows. Correspondingly, the low-frequency signals do not require small time intervals and admit a wide window extension along the time

axis. Thus wavelets well localize the low-frequency "details" on the frequency axis and the high-frequency ones on the time axis. This ability of wavelets to find a perfect compromise between the time localization and the frequency localization by automatically choosing the widths of the windows along the time and frequency axes well adjusted to their centers location is crucial for their success in signal analysis . The wavelet transform cuts up the signal (functions, operators etc) into different frequency components, and then studies each component with a resolution matched to its scale providing a good tool for time-frequency (position-scale) localization. That is why wavelets can zoom in on singularities or transients (an extreme version of very short-lived high-frequency features!) in signals, whereas the windowed Fourier functions cannot. In terms of traditional signal analysis , the filters associated with the windowed Fourier transform are constant bandwidth filters whereas the wavelets may be seen as constant relative bandwidth filters whose widths in both variables linearly depend on their positions.

The wavelet coefficients are negligible in the regions where the function is smooth. That is why wavelet series with plenty of non-zero coefficients represent really pathological functions, whereas "normal" functions have "sparse" or "lacunary" wavelet series and easy to compress. On the other hand, the Fourier series of the usual functions have a lot of non-zero coefficients, whereas "lacunary" Fourier series represent pathological functions.

## 7 Wavelets and operators

The study of many operators acting on a space of functions or distributions becomes simple when suitable wavelets are used because these operators can be approximately diagonalized with respect to this basis. Orthonormal wavelet bases provide a unique example of a basis with non-trivial diagonal, or almost-diagonal, operators. That is why wavelets, used as a basis set, allow us to solve differential equations characterized by widely different length scales found in many areas of physics and chemistry.

It is extremely important that it is sufficient to first calculate the matrix elements at some ( $j$ -th) resolution level. All other matrix elements can be obtained from it using the standard recurrence relations. As an example, we write the explicit equation for the  $n$ -th order differentiation operator.

$$\begin{aligned}
 r_k^{(n)} &= \langle \varphi(x) | \frac{d^n}{dx^n} | \varphi(x - k) \rangle = \\
 &= \sum_{i,m} h_i h_m \langle \varphi(2x + i) | \frac{d^n}{dx^n} | \varphi(2x + m - k) \rangle = \\
 &= 2^n \sum_{i,m} h_i h_m r_{2k-i-m}^{(n)}.
 \end{aligned} \tag{37}$$

It leads to a finite system of linear equations for  $r_k$  (the index  $n$  is omitted):

$$2^{-n} r_k = r_{2k} + \sum_m a_{2m+1} (r_{2k-2m+1} + r_{2k+2m-1}), \tag{38}$$

where both  $r_k$  and  $a_m = \sum_i h_i h_{i+m}$  ( $a_0 = 1$ ) are rational numbers in the case of Daubechies wavelets. The wavelet coefficients can be found from these equations up to a normalization constant. The normalization condition reads:

$$\sum_k k^n r_k = n!. \tag{39}$$

For the support region of the length  $L$ , the coefficients  $r_k$  differ from zero for  $-L + 2 \leq k \leq L - 2$ , and the solution exists for  $L \geq n + 1$ . These coefficients possess the following symmetry properties:

$$r_k = r_{-k} \quad (40)$$

for even  $n$ , and

$$r_k = -r_{-k} \quad (41)$$

for odd values of  $n$ .

At the end, two brief remarks are in order.

The analysis of any signal includes finding the regions of its regular and singular behavior. One of the main features of wavelet analysis is its capacity of doing a very precise local analysis of the regularity properties of functions. Combined with studies of Poisson equation, this approach was used for determination of a very singular potential of interaction of two uranium nuclei (see [11]).

Wavelets are well suited to reveal fractal signals. In terms of wavelet coefficients it implies that their higher moments behave in a power-like manner with the scale changing. It is well known [20] that this problem is important for multiparticle production processes which show the multifractal distribution of secondary particles in the phase space.

More detailed information about these problems can be got in [11].

## 8 Applications

Wavelets become widely used in many fields. Here we describe just two examples of wavelet application to analysis of very high multiplicity events in multihadron production and of an one-dimensional curve describing the pressure variation in gas turbines.

In multihadron production, wavelets provide a completely new way for an event-by-event analysis which is impossible with other methods because now one can distinguish specific local features of particle correlations within the available phase space. Pattern recognition at different scales becomes possible.

High energy collisions of elementary particles result in production of many new particles in a single event. Each newly created particle is depicted kinematically by its momentum vector, i.e., by a dot in the three-dimensional phase space. Different patterns formed by these dots in the phase space would correspond to different dynamics. To understand this dynamics is a main goal of all studies done at accelerators and in cosmic rays. Especially intriguing is a problem of the quark-gluon plasma, the state of matter with deconfined quarks and gluons which could exist during an extremely short time intervals. One hopes to create it in collisions of high energy nuclei. Nowadays, the data about Pb-Pb collisions are available where, in a single event, more than 1000 charged particles are produced. New data from RHIC accelerator in Brookhaven with multiplicities up to about 6000 charged particles have been already registered. LHC in CERN will provide events with up to 20000 new particles created. However we do not know yet which patterns will be drawn by the nature in individual events. Therefore the problem of phase space pattern recognition in an event-by-event analysis becomes meaningful.

In Ref. [21] the so-called continuous MHAT wavelets were first applied to analyze patterns formed in the phase space of the accelerator data on individual high multiplicity events of Pb-Pb interaction at energy 158 GeV per nucleon. The resulting pattern showed that there exist events

where many particles are concentrated close to some value of the polar angle, i.e., reveal the ring-like structure in the target diagram. The interest to such patterns is related to the fact that they can result from the so-called gluon Cherenkov radiation [22, 23] or, more generally, from the gluon bremsstrahlung at a finite length within quark-gluon medium (plasma, in particular). A cosmic ray event earlier observed in [24] initiated the discussion of this problem.

More elaborate two-dimensional analysis with Daubechies ( $D^8$ ) wavelets has been done in [25]. It confirmed these conclusions with jet regions tending to lie within some ring-like formations. Large wavelet coefficients have been found for the large-scale particle fluctuations. The resolution levels  $6 \leq j \leq 10$  were left only after the event analysis was done to store the long-range correlations in the events and get rid of short-range ones and background noise. Then the inverse restoration was done to get the event images with these dynamic correlations left only, and this is what is seen in Fig. 4. Any dot corresponds to the location of a single secondary particle on a two-dimensional polar plot, where its pseudorapidity is described by the radius and its azimuthal angle is defined around the center, as usual. The dark spots correspond to long-range correlated groups of particles (jets) restored by the abovementioned analysis. The dashed rings denote those regions of pseudorapidities which were previously suspected for some peaks in inclusive pseudorapidity distributions. It directly demonstrates that large-scale correlations chosen have a ring-like (ridge) pattern. With larger statistics, one will be able to say if they correspond to theoretical expectations. However preliminary results favor positive conclusions [25]. It is due to the two-dimensional wavelet analysis that for the first time the fluctuation structure of an event is shown in a way similar to the target diagram representation of events on the two-dimensional plot.

Let me briefly mention that some more curious patterns have been observed which, in particular, provide an information about the higher order Fourier coefficients of the azimuthal decomposition, not yet observed somewhere else.

This type of analysis has been also used in attempts to unravel in individual high multiplicity events the so-called elliptic flow which corresponds to their azimuthal asymmetry (the second Fourier coefficient different from zero). It happened that the analysis of NA49 data revealed such an asymmetry. However, it was mainly due to inhomogeneous acceptance of the detector in this experiment. This can not be cured in event-by-event analysis, and physics results can not be obtained in this way. Nevertheless, this analysis has shown that it can be used for understanding some technical problems of a particular experiment.

Another example [26] of successful application of wavelet analysis is provided by the analysis of time variation of the pressure in an aircraft compressor shown in Fig. 5. The aim of the analysis of this signal is motivated by the desire to find the precursors of a very dangerous effect (stall+surge) in engines leading to their destruction. It happened that the dispersion of the wavelet coefficients shown by the dashed line in Fig. 5 drops before the dangerous high pressure appears in the compressor of the engine. This drastic change of the dispersion can serve as a precursor of the engine destruction. No such a drop is seen in the upper dash-dotted line which shows the similar dispersion for the random signal obtained from the initial one by shuffling its values at different time. These curves show the internal correlations at the different scales existing in the primary signal possessing a very complicated structure. Even more important is the fact that the precursor helped find the physics nature of this effect. The decline of the dispersion is attributed to the dominance of a particular scale (frequency). The specific resonance is to be blamed for it. Thus the methods of preventing the engine destruction have been proposed and patented.

Let us mention that the similar procedure has been quite successful in analysis of heartbeat intervals and diagnosis of a heart disease [27, 28, 29].

The property of wavelet coefficients to be small for smooth images and large for strongly

contrasted ones has been used for the automatic focusing of microscopes [11] and corresponding deciphering of some bad quality blood samples in medical research.

Both the direct and inverse wavelet transforms have to be applied for image compression, its further transmission and restoration. This becomes especially important if the capacity of the transmission line is rather low. One of the examples of such a procedure and its comparison with windowed Fourier transform are demonstrated in [11].

Many other examples can be found in the cited literature and in Web sites.

## 9 Conclusions

The beauty of the mathematical construction of the wavelet transformation and its utility in practical applications attract researchers from both pure and applied science. We especially emphasize here that wavelet analysis of multiparticle events in high energy particle and nucleus collisions proposes a completely new approach to the effective event-by-event study of patterns formed by secondary particle locations within the available phase space. The newly found patterns have already shown some specific dynamical features not discovered before. One can expect for other surprises when very high multiplicity events obtained in detectors with good acceptance will become available for analysis .

Moreover, the commercial outcome of this research has become quite important. We have outlined a minor part of the activity in this field. However we hope that the general trends in the development of this subject became comprehended and appreciated.

### Acknowledgments

This work has been supported in part by the RFBR grants N 02-02-16779, 03-02-16134, NSH-1936.2003.2.

### Figure Captions

Fig. 1. The histogram and its wavelet decomposition.

The initial histogram is shown in the upper part of the Figure. It corresponds to the level  $j = 4$  with 16 bins (Eq. (1)). The intervals are labelled on the abscissa axis at their left-hand sides. The next level  $j = 3$  is shown below. The mean values over two neighboring intervals of the previous level are shown at the left-hand side. They correspond to eight terms in the first sum in Eq. (4). At the right-hand side, the wavelet coefficients  $d_{3,k}$  are shown. Other graphs for the levels  $j = 2, 1, 0$  are obtained in a similar way. The transitions from  $s$ -coefficients to  $d$ -coefficients of coarser levels are depicted by arrows.

Fig. 2. The Haar scaling function  $\varphi(x) \equiv \varphi_{0,0}(x)$  and "mother" wavelet  $\psi(x) \equiv \psi_{0,0}(x)$ .

Fig. 3. Daubechies scaling functions (solid lines) and wavelets (dotted lines) for  $M = 2, 4$ .

Fig. 4. The restored image of long-range correlations (dark regions) on experimental plot of points in polar coordinates corresponding to pseudorapidities and azimuthal angles of 1029 charged particles produced in a single event of central Pb-Pb interaction at 158 GeV.

It clearly displays the typical ring-like structure of jetty spots. The dashed rings are drawn according to preliminary guesses based on spikes in inclusive pseudorapidity distribution for this event.

The two rings correspond to two symmetrical forward-backward regions in the center of mass system. One would interpret this image as jets which tend to be emitted by both colliding nuclei at the same (in the corresponding hemispheres) fixed polar angle that is typical for Cherenkov radiation.

Fig. 5. The pressure variation in the compressor of a gas turbine measured each millisecond during 5 sec with a drastic increase at the end. The signal of the pressure sensor is shown by the quite irregular solid line.

The time dependence of the pressure in the engine compressor has been wavelet analyzed. The dispersion of the wavelet coefficients (the dashed line) shows the maximum and the remarkable drop about 1 sec prior the drastic increase of the pressure providing the precursor of this malfunction. The shuffled set of the data does not show such an effect for the dispersion of the wavelet coefficients (the upper curve) pointing to its dynamic origin.

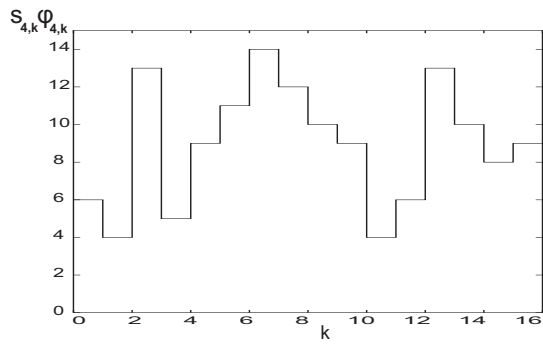
## References

- [1] Meyer, Y., *Wavelets and Operators*, Cambridge: Cambridge University Press, 1992.
- [2] Daubechies, I., *Ten Lectures on Wavelets*, Philadelphia: SIAM, 1991.
- [3] Y. Meyer, Y., and Coifman, R., *Wavelets, Calderon-Zygmund and multilinear operators*, Cambridge: Cambridge University Press, 1997.
- [4] Meyer, Y., *Wavelets: Algorithms and Applications*, Philadelphia: SIAM, 1993.
- [5] *Progress in Wavelet Analysis and Applications*, Eds. Meyer, Y., and Roques, S., Gif-sur-Yvette: Editions Frontieres, 1993.
- [6] Chui, C.K., *An Introduction to Wavelets*, San Diego: Academic Press, 1992.
- [7] Hernandez, K., and Weiss, G., *A First Course on Wavelets*, Boca Raton: CRC Press, 1997.
- [8] Kaiser, G., *A Friendly Guide to Wavelets*, Boston: Birkhauser, 1994.
- [9] *Wavelets: An Elementary Treatment of Theory and Applications*, Ed. Koornwinder, T., Singapore: World Scientific, 1993.
- [10] Astafyeva, N.M., *Physics-Uspekhi*, 1996, vol. 39, p. 1085.
- [11] Dremin, I.M., Ivanov, O.V., and Nechitailo, V.A., *Physics-Uspekhi*, 2001, vol. 44, p. 447.
- [12] *Wavelets in Physics*, Ed. Van den Berg, J.C., Cambridge: Cambridge University Press, 1998.
- [13] Mallat, S., *A Wavelet Tour of Signal Processing*, New York: Academic Press, 1998.
- [14] Erlebacher, G., Hussaini, M.Y., and Jameson, L.M., *Wavelets Theory and Applications*, Oxford: Oxford University Press, 1996.
- [15] *Wavelets in Medicine and Biology*, Eds. Aldroubi, A., and Unser, M., Boca Raton: CRC Press, FL, 1994.

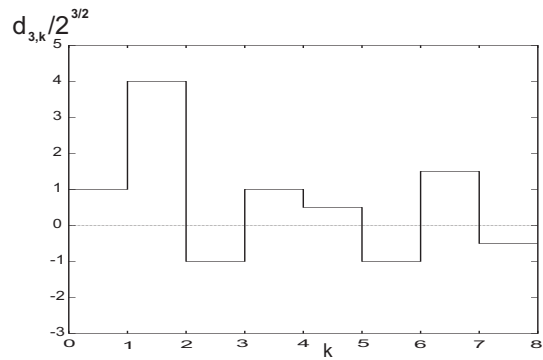
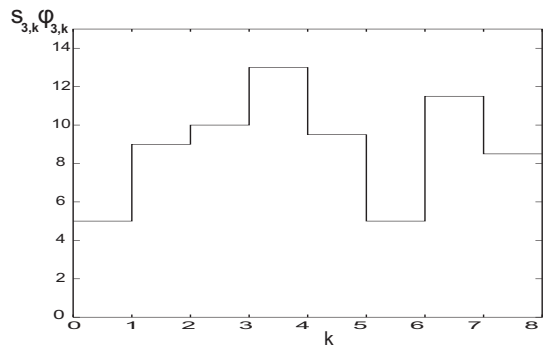
- [16] Carmona, R., Hwang, W.-L., and Torresani, B., *Practical Time-Frequency Analysis*, San Diego: Academic Press, 1998.
- [17] Grossman, A., and Morlet, J., in *Mathematica+Physics, Lectures on Recent Results*, Vol. 1, Ed. Streit, L., Singapore: World Scientific, 1985.
- [18] Morlet, J., Arens, G., Fourgeau, E., and Giard, D., *Geophysics*, 1982, vol. 47, pp. 203, 222.
- [19] Haar, A., *Math. Ann.*, 1910, vol. 69, p. 331.
- [20] De Wolf, E.A., Dremin, I.M., and Kittel, W., *Phys. Rep.*, 1996, vol. 270, p. 1.
- [21] Astafyeva, N.M., Dremin, I.M., and Kotelnikov, K.A., *Mod. Phys. Lett. A* 1997, vol. 12, p. 1185.
- [22] Dremin, I.M., *JETP Lett.*, 1979, vol. 30, p. 140.
- [23] Dremin, I.M., *Yad. Fiz.*, 1981, vol. 33, p. 1357.
- [24] Apanasenko, A.V., Dobrotin, N.A., Dremin, I.M., et al., *JETP Lett.* 1979, vol. 30, p. 145.
- [25] Dremin, I.M., Ivanov, O.V., Kalinin, S.A., et al., *Phys. Lett. B*, 2001, vol. 499, p. 97.
- [26] Dremin, I.M., Furletov, V.I., Ivanov, O.V., et al., *Control Engineering Practice*, 2002, vol. 10, p. 599.
- [27] Thurner, S., Feurstein, M.C., and Teich, M.C., *Phys. Rev. Lett.*, 1998, vol. 80, p. 1544.
- [28] Amaral, L.A.N., Goldberger, A.L., Ivanov, P.C., et al., *Phys. Rev. Lett.*, 1998, vol. 81, p. 2388.
- [29] Ivanov, P.C., Amaral, L.A.N., Goldberger, A.L., et al., *Nature*, 1999, vol. 399, p. 461.



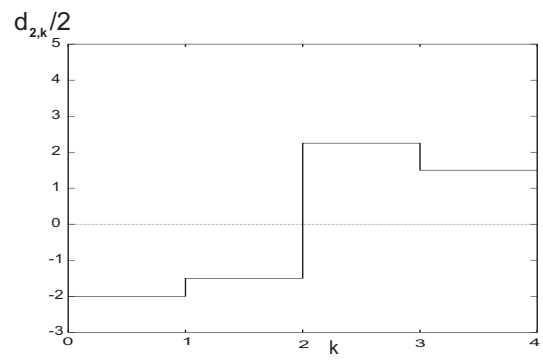
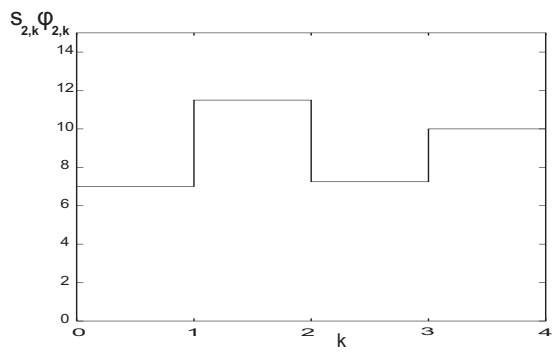
j



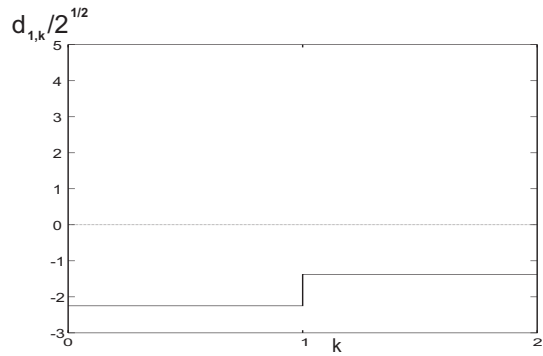
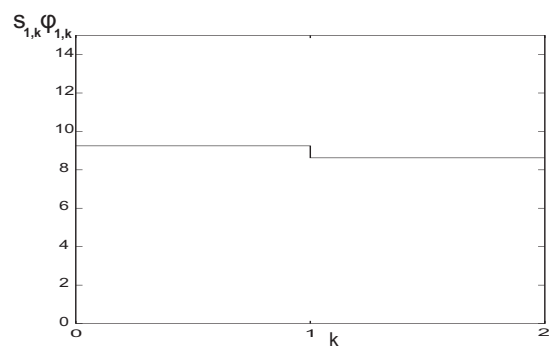
4



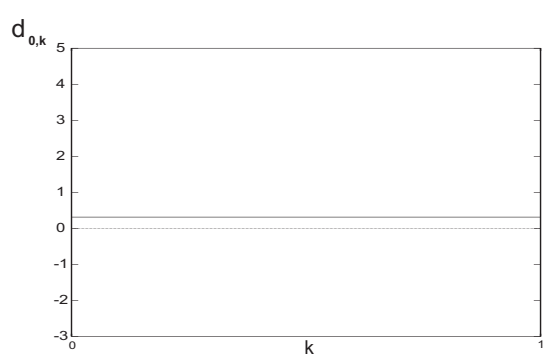
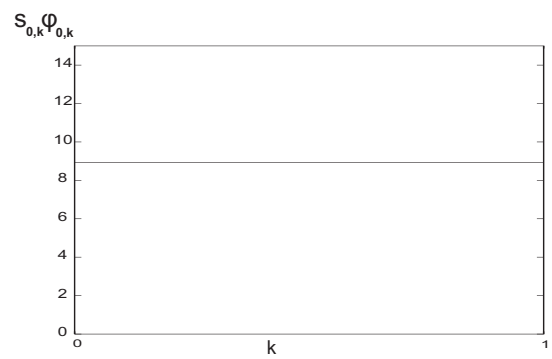
3



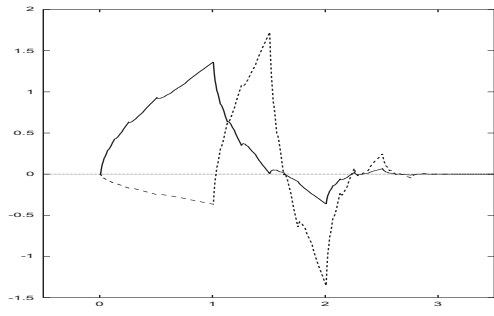
2



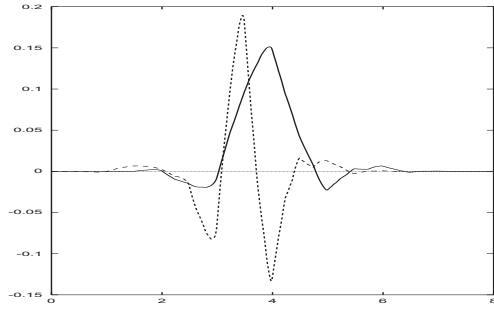
1



0



$M=2$



$M=4$

